POLITECNICO DI TORINO
Repository ISTITUZIONALE

Hollow vortices and wakes past Chaplygin cusps

(Article begins on next page)

20 April 2024

Hollow vortices and wakes past Chaplygin cusps

Luca Zannetti and Davide Lasagna

Politecnico di Torino, DIMEAS, Torino, Italy
luca.zannetti@polito.it, davide.lasagna@polito.it

Abstract

By using analytic tools for 2D rotational inviscid flow, the stagnation points of Pocklington hollow vortices are replaced by Chaplygin cusps, that is, by regions of fluid at rest. By solidifying the bounding free streamlines, solid bodies are obtained along whose walls adverse pressure gradients are avoided. These results are relevant to the theory and practice of control of separated flow at high Reynolds number. Examples are presented pertinent to single bodies and cascade of bodies which trap hollow vortices or generate open hollow wakes.

Key words: hollow vortices, separated flow, complex analysis

1. Introduction

According to the Stepanov theorem ([1],[2],[3]), the pressure gradient cannot be everywhere favorable on a body immersed in a 2D steady potential flow; as a consequence, in the limit of the Reynolds number going to infinity, it is not possible to design a body which prevents flow separation from its smooth walls by avoiding adverse pressure gradients.

As argued in [3], the Stepanov theorem does not hold if vorticity affects the flow field, and one could think of properly designed bodies in which a steady rotational separated flow hinders other uncontrolled secondary separations by averting adverse gradients. The idea of bodies which trap free vortices is based on this concept and in [3],[4] examples of such bodies have been provided. In those examples the separating streamline leaves the body from a cusped edge and the separated flow is modeled as a finite region of flow entrained by a point vortex trapped on an equilibrium location.

Figure 1 shows an example from [4], where two cusped solid bodies capture a vortex pair. It has been obtained by exploiting the Chaplygin's idea that stagnation points can, in general, be replaced by regions of fluid at

rest bounded by free streamlines (see [5], [6]). Since in a stagnation region pressure is constant, solidification of those streamlines provides solid bodies free from adverse gradients.

We adopt here a different model for the separated flow which includes the case of an infinite wake. In general, the 2D steady rotational inviscid flow is governed by the equation $\nabla^2\psi = -\omega(\psi)$, where ω and ψ represent vorticity and stream function. As shown by Batchelor [7], [8], in the inviscid limit as the Reynolds number goes to infinity, the steady separated flow is a vortex patch bounded by a vortex sheet, that is, the governing equation becomes

$$\nabla^2\psi = -\omega \mathrm{H}(\alpha - \psi) + B\,\delta(\alpha - \psi), \tag{1}$$

with H denoting the Heaviside step function, δ the Dirac delta function and where α and B are the values of the stream function and of the jump of the Bernoulli constant at the patch boundary, respectively. In the Batchelor flow, α is the value of the stream function on the separating streamline and, as shown by Chernyshenko [9], the values of ω and B are defined by the location of the separation point and by the constraint that the boundary-mixing layer around the separated flow has to be cyclic.

By loosening the requirement that the inviscid solution has to be the viscous limit for $Re \to \infty$, different values of α, B, ω can be selected which yield multiple solutions. Even though the physical meaning is weakened, these solutions are interesting for they include the genuine Batchelor flow. The main advantage is that they allow very accurate solutions in a way which is simpler than the genuine Batchelor flow. For instance, the choice $|\alpha| = \infty$ yields the point vortex model, and the choice $B = 0$ yields a two parameter (α, ω) family of vortex patch solutions as, for instance, in [10], [11].

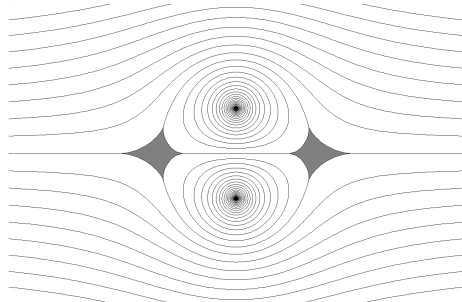The "hollow" model is here adopted by assuming $\omega = 0$; in this model

Figure 1: Chaplygin cusps replacing the stagnation points of a vortex pair flow.
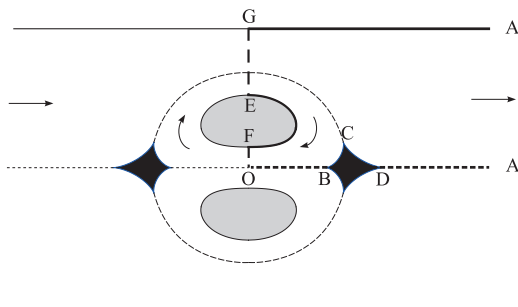
2

Figure 2: Chaplygin cusps in a channel trapping a closed hollow vortex pair ($q_h = 4.5$, $q_c = 0.5$, $\tau_G = 3$).

the vorticity is concentrated on a vortex sheet which bounds a region of fluid at rest. It follows that the vortex sheet reduces to a free streamline with constant velocity q_h and that the Bernoulli jump B reaches its maximum allowable value $B = q_h^2/2$. This flow model has been known for a long time, for instance, it was adopted by Pocklington's [12] and Michell's [13] who used the hodograph-plane method to define the geometry of finite hollow vortices and infinite hollow regions standing above a flat plane. Lavrentiev [14] suggested to use it to model the wake past bluff bodies, as in [15], [16], [17]. Further examples of the hollow vortex concept are presented, for instance, in [18],[19].

An example of solution based on this model is shown in figure 2, where, in a way similar to figure 1, the stagnation points of a cascade of Pocklington vortex pairs have been replaced by Chaplygin cusps. The separated flow consists of a pair of hollow vortices, that is a pair of regions with a core of fluid at rest encircled by a layer of potential flow.

A further example is shown in figure 3, where Chaplygin cusps replace the stagnation points of a cascade of infinite Pocklington hollow regions. As above, the wake consists of infinite hollow cores bounded by a layer of potential flow. It should be noted that the hollow model is richer than the point vortex model, which is characterized by closed streamlines and, as a consequence, is unable to model an infinite wake.

In Sec. 2 the Pocklington solutions for finite and infinite hollow regions is recalled and extended to the case of cascade or, in equivalent way, channel flow. In Sec. 3 the Chaplygin cusps are introduced and examples of solutions are described. Concluding remarks are drawn in Sec. 4.
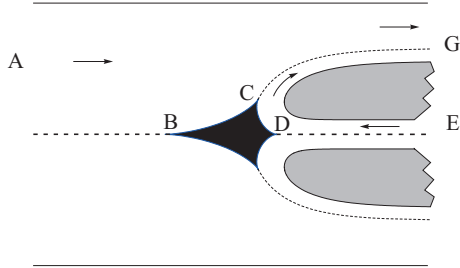
3

Figure 3: Open hollow wake past a cascade of Chaplygin cusps ($q_h = 3$, $q_c = 0.8$).

2. The Pocklington's solutions

For 2D potential flows, the inverse problem of determining the shape of streamlines along which the velocity distribution is prescribed can in general be solved by the hodograph-plane method.

The method consists on determining the analytic function $z(\lambda)$ which maps a suitably chosen canonical domain of the parameter λ-plane onto the flow domain of the physical z-plane. Briefly, it is based on exploiting the chain rule $\mathrm{D}\{w(z(\lambda))\} = w'(z)z'(\lambda)$, rearranged as

$$\frac{\mathrm{d}z}{\mathrm{d}\lambda} = \frac{\mathrm{d}w/\mathrm{d}\lambda}{\mathrm{d}w/\mathrm{d}z}, \tag{2}$$

where $z = x + \mathrm{i}\,y$ is the complex coordinate of the physical z-plane, w is the complex potential and λ is the complex coordinate of the parameter plane.

Let $\tau = \mathrm{d}w/\mathrm{d}z$ be the complex coordinate of the hodograph $\mathrm{d}w/\mathrm{d}z$-plane. The shape of the flow field boundary in the τ-plane, that is, the velocity distribution along the boundary, is provided by the formulation of the inverse problem. The solution is obtained by expressing the right-hand side of (2) as an explicit function of λ. The denominator $\mathrm{d}w/\mathrm{d}z$ is expressed as function of λ by conformally mapping the domain of the τ-plane onto a canonical domain of the parameter λ-plane, while the the numerator $\mathrm{d}w/\mathrm{d}\lambda$ can be defined by elementary means, as the examples below show. The mapping function $z(\lambda)$ is finally obtained by analytical or numerical integration.

The canonical domain of the λ-plane can be arbitrarily chosen. For a simply connected flow domain, it could typically be a half-plane or a circle or a rectangle. As a consequence, different mapping functions $z(\lambda)$ can be defined. This leads to different processes to reach the solution, which, in any case, is unique. In fact, as required by the Riemann mapping theorem, the
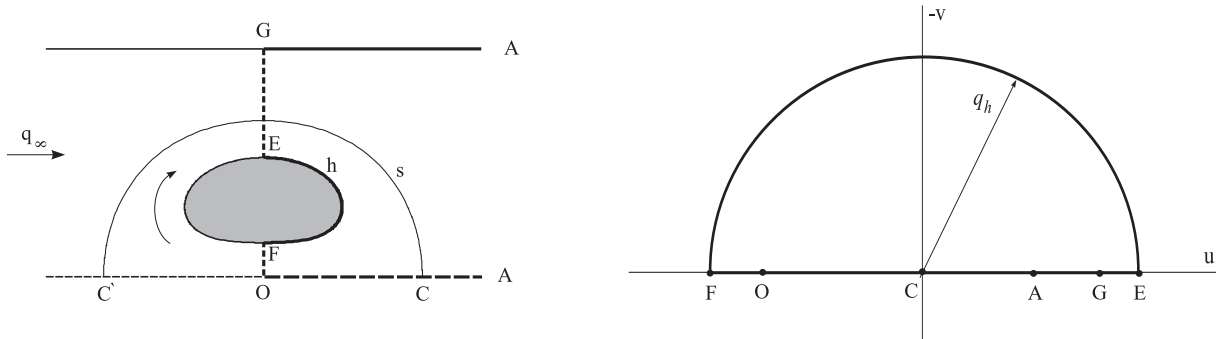
Figure 4: Left: Hollow vortex pair in a channel. Right: Hodograph-plane $(\mathrm{d}w/\mathrm{d}z = u - iv)$.

different canonical domains can be mapped onto each other. A large number of examples and variations of the method can be found in the literature, Gurevich [6], for instance, is a rich source on this matter.

2.1. Pocklington's hollow vortex pair

As an example of the procedure, we retrace the Pocklington [12] solution (see also [20],[21]), with some variation relevant to the problems dealt with in Sec. 3.

The flow considered by Pocklington consists of a pair of hollow vortices standing in equilibrium in an asymptotically uniform flow. We consider the more general flow past a cascade of pairs of hollow vortices or, equivalently, of a vortex pair in a channel. For the channel width going to infinity, the present flow coincides with the Pocklington one.

Figure 4 shows the upper vortex, where h denotes the vortex sheet bounding the hollow body of fluid at rest and s is the separatrix that divides the body of fluid entrained by the vortex from the fluid flowing along the channel. Due to symmetry, the problem of determining the hollow shape can be restricted to the study of the region $ACOFEGA$, marked by thick lines, with A located at the downstream infinity. The relevant pattern of the hodograph τ-plane is shown on the right-hand side of the figure, where q_h is the velocity along the hollow boundary.

Let the flow be normalized by assuming as reference velocity the velocity at infinity (A) and as reference length the half width of the channel. Hence, in the hodograph plane $\tau_A = 1$ and, being C a stagnation point, $\tau_C = 0$. As discussed below, the velocity on the hollow boundary q_h and the velocity τ_G are free parameters, while the velocity τ_O is a parameter to be adjusted to assure the closure of the hollow.
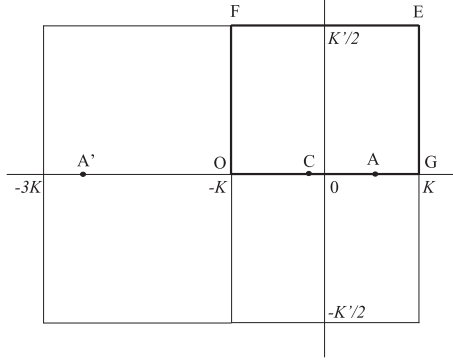
5

Figure 5: λ-plane.

The semicircle of the τ-plane is mapped onto the rectangle marked by thick lines in fig. 5. First, the semicircle of the τ-plane is mapped onto a semicircle of the intermediate μ-plane by the Möbius mapping

$$\mu = -b\frac{\tau - a\,\tau_E}{a\,\tau - \tau_E},\tag{3}$$

with a, b such that $\mu_G = -\mu_O = 1$ and $\mu_F = -\mu_E$. Then, the mapping onto the rectangle of the λ-plane is given by $\mu = \operatorname{sn}(\lambda, m)$, where "sn" is the Jacobi sine amplitude function. The parameter m is obtained by solving by iteration the implicit equation

$$\mu_E = \operatorname{sn}[K(m) + \mathrm{i}\,K'(m)/2, m],$$

where K denotes the complete elliptic integral of the first kind and $K'(m) = K(1 - m)$. Finally, by inverting eq. (3), the function $\tau(\lambda)$ results as

$$\tau = \frac{\mathrm{d}w}{\mathrm{d}z} = \tau_E\,\frac{a\,b + \operatorname{sn}(\lambda, m)}{b + a\operatorname{sn}(\lambda, m)}.\tag{4}$$

As inferred by the requirement that the sides FE and OG are streamlines and by the symmetry properties of the flow field, the complex velocity $\mathrm{d}w/\mathrm{d}\lambda$ has to be a doubly periodic function of λ, with half periods $\omega = 2K$ and $\omega' = \mathrm{i}\,K'/2$. In the periodic domain, shown in fig. 5), it has to have two first order poles, located at λ_A (downstream infinity) and $\lambda_{A'} = -(\lambda_A + \omega)$ (upstream infinity), which represent the sink and the source responsible for the mass flow streaming inside the channel. Thus, $\mathrm{d}w/\mathrm{d}\lambda$ is expressed by the elliptic function

$$\frac{\mathrm{d}w}{\mathrm{d}\lambda} = Q\left[\zeta(\lambda - \lambda_{A'}) - \zeta(\lambda - \lambda_A) + \kappa\right],\tag{5}$$

6

where ζ is the Weierstrass ζ-function, and Q and κ are constants to be determined. For the sake of brevity, the dependence of the Weierstrass functions on the half-periods (ω, ω') has been omitted. According to eq. (2), Q has the mere meaning of scale factor which can be adjusted a posteriori to enforce the channel width, while the value of κ is defined by the condition that C is a stagnation point, that is $(\mathrm{d}w/\mathrm{d}\lambda)_C = 0$, which yields

$$\kappa = \zeta(\lambda_C - \lambda_A) - \zeta(\lambda_C - \lambda_{A'}).$$

The closure of the hollow implies that $\oint_h \mathrm{d}z = 0$. Due to the symmetry of the hollow with respect to the imaginary axis, this condition reduces to the scalar equation

$$\mathrm{Re} \int_F^E \frac{\mathrm{d}z}{\mathrm{d}\lambda} \mathrm{d}\lambda = 0.$$

By means of a trial and error process, for a choice of q_h and τ_G, this equation is used to determine the value of τ_O.

The problem has thus two degrees of freedom, represented by the free choice of q_h and τ_G. The physical soundness of this outcome can be deduced by considering that in a channel with a given width there is a single infinity of solutions for point vortices $(q_h \to \infty)$ standing in equilibrium with different values of the circulation γ, and that each point vortex can be desingularized into a family of hollow vortices with the same circulation γ and different velocity q_h at the hollow boundary. The value of the hollow circulation is given by $\gamma = 2(w_E - w_F)$, where, by integrating eq. (5), the complex potential w is

$$w = Q \left[\log \frac{\sigma(\lambda - \lambda_{A'})}{\sigma(\lambda - \lambda_A)} + \kappa \lambda \right],$$

with σ denoting the Weierstrass σ-function.

An example of hollow vortex solution is shown in figure 6, corresponding to the choice $q_h = 4.5$, $\tau_G = 3$, which yields $\tau_O = -4.277$ and $\gamma = -7.806$. The figure also shows the location of the point vortex which stands in equilibrium with the same circulation γ.

The vortex pair considered by Pocklington stands in an unbounded domain. According to the above analysis, it corresponds to choose $\tau_G = \tau_A = 1$, which yields $\lambda_A = \omega/2$ and $\lambda_A - \lambda_{A'} = 2\omega$. As a consequence of the 2ω period of $\mathrm{d}w/\mathrm{d}\lambda$, the source and sink that, according to eq. (5), are located in $\lambda_{A'}$ and λ_A, merge into a doublet which expresses the asymptotic flow in the physical plane. Thus, eq. (5) is replaced by

$$\frac{\mathrm{d}w}{\mathrm{d}\lambda} = Q \left[\wp(\lambda - \lambda_A) + \kappa \right],$$
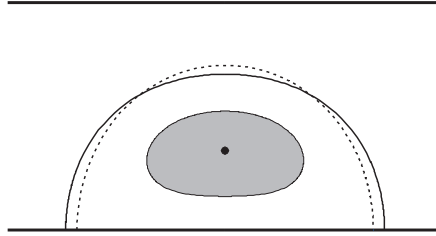
7

Figure 6: Hollow vortex ($q_h = 4.5$) and point vortex standing in equilibrium with $\gamma = 1.735$. Solid line: hollow vortex separatrix; dotted line: point vortex separatrix.

with $\kappa = -\wp(\lambda_C - \lambda_A)$, where $\wp$ is the Weierstrass $\wp$-function. By integration, the complex potential becomes

$$w = Q\left[-\zeta(\lambda - \lambda_A) + \kappa\,\lambda\right].$$

Let the problem be normalized by assuming as reference velocity the velocity at infinity and as reference circulation the absolute value of the vortex circulation $|\gamma|$. Since, as above, $\gamma = 2(w_E - w_f)$, Q is given by

$$Q = 1/\{2[\zeta(\lambda_E - \lambda_A) - \zeta(\lambda_F - \lambda_A) - k(\lambda_E - \lambda_F)]\}$$

2.2. Pocklington's open hollow region

Pocklington [12] extended the above solution to hollows which extends to the downstream infinity. This solution can be assumed as the basis to model a wake which extends to infinity. As above, this solution is here derived in different form and generalized to the case of the flow inside a 2D channel.

A solution is shown in figure 7, where the flow on the upper half channel is presented. By solidifying the symmetry line, it can be seen as an infinite separated flow which detaches at point C and consists of an infinite hollow region bounded by a layer of potential flow; as above, the vorticity is concentrated on the vortex sheet bounding the hollow. The flow field is characterized by a jet streaming from E in a direction opposite to the main flow. The jet is arrested at C and turns around the hollow. The downstream asymptotic pressure should be uniform and equal to the pressure inside the hollow and, as a consequence, at downstream infinity, the recirculating jet flow and the main flow should attain the velocity q_h of the hollow boundary.

The relevant hodograph τ-plane ($\tau = \mathrm{d}w/\mathrm{d}z$) is shown on the left-hand side of figure 8. The semicircle GE represents the constant flow speed q_h along the hollow boundary. The line ACE represents the flow velocity along the channel centerline and the line AG is relevant to the upper wall. The
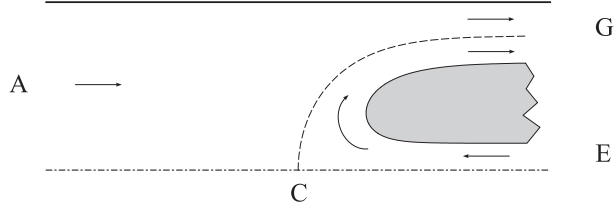
Figure 7: Open hollow wake and separatrix($q_h = 5$).

interior of the semidisc represents the flow velocity inside the channel, it is mapped onto the upper half λ-plane by the transformation

$$\tau = q_h \frac{1 - \sqrt{\lambda}}{1 + \sqrt{\lambda}}, \tag{6}$$

which is such that the hollow boundary is mapped onto the negative real axis and the channel walls onto the positive real axis.

The complex potential in the transformed λ-plane consists of a source located in λ_A, with Q_A mass flow responsible for the flow running in the channel from the upstream infinity A, and by a sink located in $\lambda = \lambda_G = 0$, with mass flow is $Q_G = Q_A + Q_E$, where Q_E represents the mass flow streaming from E to G. The complex velocity in the λ-plane is thus

$$\frac{\mathrm{d}w}{\mathrm{d}\lambda} = \frac{Q_A}{2\pi} \left(\frac{1}{\lambda - \lambda_A} - \frac{Q_G}{Q_A} \frac{1}{\lambda} \right). \tag{7}$$

By taking the upstream velocity q_A as reference velocity and the half width of the channel as reference length, $Q_A = 2$. By enforcing that $\lambda = \lambda_C = 1$ is a stagnation point, one obtains $Q_G/Q_A = 1/(1 - \lambda_A)$. Thus, according to eq. (2), the derivative of the $z = z(\lambda)$ mapping is given by

$$\frac{\mathrm{d}z}{\mathrm{d}\lambda} = \frac{\mathrm{d}w/\mathrm{d}\lambda}{\tau} = \frac{1}{\pi\, q_h} \left[\frac{1}{\lambda - \lambda_A} - \frac{1}{\lambda(1 - \lambda_A)} \right] \frac{1 + \sqrt{\lambda}}{1 - \sqrt{\lambda}},$$

whose integration yields

$$z = \frac{\lambda_A(\lambda - 1)[-5 + 4\sqrt{\lambda} + \lambda + 4\log(\sqrt{\lambda} - 1)]}{\pi\, q_h\, \lambda(\lambda_A - \lambda)(\lambda_A - 1)}$$

For the above normalization, $\tau_A = 1$, which, according to eq. (6) yields $\lambda_A = [(q_h - 1)/(q_h + 1)]^2$. The problem has thus one degree of freedom expressed by the free choice of $q_h \geq 1$.
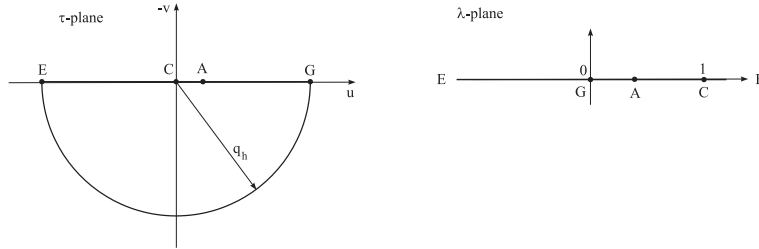
9

Figure 8: Hodograph τ-plane and transformed λ-plane.

An example of solution is shown in fig. 7 for $q_h = 5$. The boundary of the hollow and the upper wall and centerline of the channel are the z-image of the real axis of the λ-plane, while the separatrix is the z-image of the $\psi = const$ streamline which departs from the stagnation point $\lambda = \lambda_C = 1$.

The flow in an unbounded domain corresponds to the choice $q_h = 1$. In this case, $\tau_G = \tau_A = 1$, and, in the λ-plane, $\lambda_A = \lambda_G = 0$. By the merging of the source located in λ_A and the sink located in λ_G into a doublet located in $\lambda = 0$, the above expression (7) for the complex velocity is changed in

$$\frac{\mathrm{d}w}{\mathrm{d}\lambda} = \frac{Q}{2\pi}\left(\frac{1}{\lambda^2} - \frac{1}{\lambda}\right).$$

where Q is a free parameter which defines the arbitrary length scale of the solution.

3. Chaplygin cusps

Following the same reasoning as in [4], the stagnation points C of the above Pocklington flows can be replaced by Chaplygin cusps, that is, by finite regions filled by fluid at rest. As below described, the hodograph-plane method is particularly well suited to obtain these solutions. Beside the general interest on analytical or almost analytical solution of non trivial flows governed by the Euler equations, there is also some physical interest on this study. In fact, as for the hollow vortices, the Chaplygin cusps are characterized by constant pressure, that is, by constant velocity along their boundary. Let the cusp be considered as solid bodies and the channel as the periodic domain of a cascade flow, the resulting flow possesses the re-markable property, discussed in Sec. 1, that there are no adverse pressure gradients along any solid bounding wall.
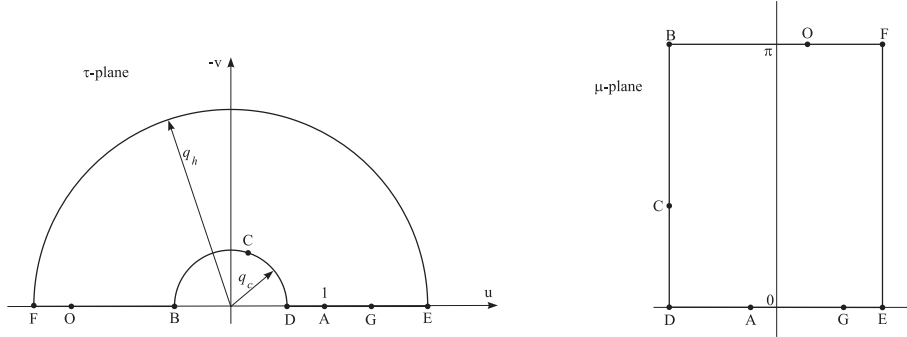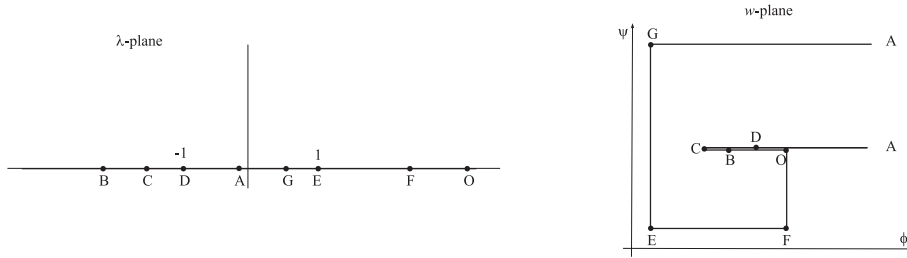
Figure 9: Hodograph τ-plane and intermediate μ-plane.

Figure 10: Transformed λ-plane and complex-potential w-plane.

3.1. Chaplygin cusps and hollow vortices

We replace the stagnation points C and C' of figure 4 by a pair of Chaplygin cusps, that is, dead-flow regions with finite area. The solution is shown in figure 2.

The problem is normalized by assuming the flow velocity at infinity and the distance between the upstream and downstream cusps as reference velocity and length, respectively. Due to the symmetry of the flow field with respect to the real and imaginary axis, the solution can be obtained for the domain marked by thick lines on figure 2. The relevant pattern of the complex velocity in the hodograph τ-plane is shown in figure 9. The solution is obtained by mapping the inside of this figure onto the upper half-λ-plane (figure 10). To this purpose, the figure is first mapped into a rectangle of the intermediate μ-plane (figure 9) by the transformation

$$\mu = \log\left(\frac{\tau}{\sqrt{\tau_E \, \tau_D}}\right),$$

then the interior of the rectangle is mapped onto the the upper half-λ-plane

11

by the elliptic sine-amplitude function

$$\lambda = \mathrm{sn}\left(\frac{K(m)}{\mu_E}\mu\,,\,m\right),$$

where $K(m)$ is the complete elliptic integral of the first kind and, according to the implicit equation $K(m)/K(1-m) = \mu_E/\pi$, the parameter m is defined by the rectangle aspect ratio μ_E/π.

The $\lambda \to \tau$ mapping is therefore given by:

$$\tau = \sqrt{\tau_E\,\tau_D}\,\exp\left[\frac{\mu_E}{K(m)}\mathrm{sn}^{-1}(\lambda,m)\right]$$

The complex velocity $\mathrm{d}w/\mathrm{d}\lambda$ can be expressed by considering the right-hand side of figure 10, which shows the pattern of the complex potential w along the path marked by thick lines in the physical z-plane (fig. 2). It results in a polygon which is mapped onto the upper half-λ-plane by the Schwarz-Christoffel mapping, which yields:

$$\frac{\mathrm{d}w}{\mathrm{d}\lambda} = -\kappa\frac{\lambda - \lambda_C}{(\lambda - \lambda_A)\sqrt{\lambda - \lambda_G}\sqrt{\lambda - \lambda_F}\sqrt{\lambda - \lambda_E}\sqrt{\lambda - \lambda_D}}. \tag{8}$$

where $|\kappa|$ is a parameter which defines the geometrical scale and can be set a posteriori.

The derivative $\mathrm{d}z/\mathrm{d}\lambda$ (eq. 2) is thus determined as a function of λ and the solution is obtained by its numerically integration.

The problem depends on five real parameters, namely q_h, q_c, τ_G, τ_O, $\varphi_C = \arg(\tau_C)$. The requirement that the hollow boundaries and the Chaplygin bodies have to be closed sets two constraints. As consequence of the symmetry of the solution, these constraints are expressed by the two real equations

$$\mathrm{Re}\int_E^F \frac{\mathrm{d}z}{\mathrm{d}\lambda}\mathrm{d}\lambda = 0, \qquad \mathrm{Im}\int_B^D \frac{\mathrm{d}z}{\mathrm{d}\lambda}\mathrm{d}\lambda = 0.$$

The problem has thus three degrees of freedom. Our choice was to select as free parameters q_h, q_c and τ_G, and to let τ_O and φ_C be determined by the fulfillment of the constraints. The parameters $q_h < 1$, $0 < q_c < 1$ have a primary effect on defining the sizes of the hollows and Chaplygin bodies, while the primary effect of $\tau_G \geq 1$ is on the channel width.

For $\tau_G = \tau_A = 1$ the complex potential pattern is changed as shown in figure 11 and the above solution degenerates to a channel with an infinite width, that is, to an unbounded domain with a single pair of Chaplygin
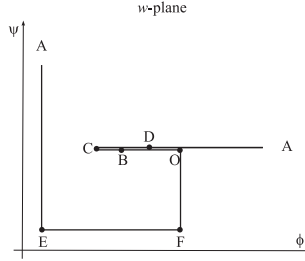
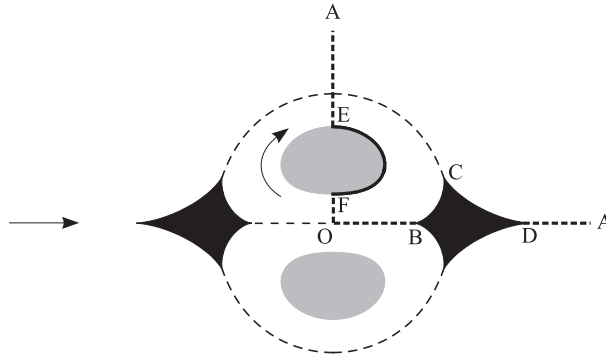Figure 11: Complex-potential w-plane for $\tau_G = \tau_A = 1$.

Figure 12: Chaplygin cusps in an unbounded domain ($q_h = 3$, $q_c = 0.5$).

cusps. By defining a new Schwarz-Christoffel mapping, we see that the above solution still holds by just replacing λ_G with λ_A in eq. (8), which becomes

$$\frac{\mathrm{d}w}{\mathrm{d}\lambda} = -\kappa \frac{\lambda - \lambda_C}{(\lambda - \lambda_A)^{3/2}\sqrt{\lambda - \lambda_F}\sqrt{\lambda - \lambda_E}\sqrt{\lambda - \lambda_D}}.$$

An example of solution for a single pair of Chaplygin cusps is shown in figure 12, corresponding to the choice $q_h = 3$, $q_c = 0.5$.

3.2. Chaplygin cusps and open hollow wakes

The cascade of Chaplygin cusps with infinite hollow wakes shown in figure 3 has been obtained by replacing the stagnation point C of the infinite Pocklington hollow shown in figure 7. The pertinent hodograph plane is the half-annulus traced on the left of figure 13.

As above, the flow is normalized by the body length and by the upstream velocity $\tau_A = 1$. The hodograph, which depends on two free parameters, namely, the $0 < q_c < 1$ velocity on the cusp and the q_h velocity on the hollow core of the wake, is mapped by $\lambda = \log \tau$ onto the rectangle marked

13

by thick lines on the right-hand side of figure 13. The sides of the rectangle correspond to streamlines, as a consequence, the complex velocity $dw/d\lambda$ has to be a doubly periodic function, with half periods $\omega = \log q_h/q_c$ and $\omega' = i\pi$. The relevant periodic domain is traced by dotted lines on figure 13. Let Q_A be the mass flow flowing from upstream in the channel and Q_E the mass flow running from E to G in the wake potential layer, the complex velocity $dw/d\lambda$ has to present a source with Q_A mass flow located in $\lambda_A = 0$, a source with Q_E mass flow located in $\lambda_E = -\log q_h$, a sink with $Q_A + Q_E$ mass flow located in $\lambda_G = \log q_h$ plus their infinite reflections with respect the thick rectangle sides. Enforcing the double periodicity with respect the dotted rectangle, the complex velocity is thus the elliptic function

$$
\begin{aligned}
\frac{dw}{d\lambda} =& \frac{Q_A}{2\pi} \left\{ \zeta(\lambda) - 2\zeta(\lambda - \lambda_G) + \zeta(\lambda - \lambda_{A'}) \right. \\
& \left. + \frac{1}{2}Q_E/Q_A[\zeta(\lambda - \lambda_E) - \zeta(\lambda - \lambda_G)] + i\kappa \right\},
\end{aligned}
\tag{9}
$$

with $\lambda_{A'} = 2\lambda_G$ and where ζ is the Weierstrass ζ function. Q_A plays the role of a scale factor and it is adjusted a posteriori to make unit the length of the cusped body. The values of the mass flow ratio Q_E/Q_A and of the constant κ are determined by enforcing that $(dw/d\lambda)_B = (dw/d\lambda)_C = 0$. In fact, the condition that the sides of the rectangle of the λ-plane are streamlines implies that the corner B has to be a stagnation point, and C is, as well, a stagnation point for it is the λ-image of the separation location. Let $\lambda_C = \log q_c + i\varphi_c$, the value of φ_c is not known a priori, it is determined by enforcing the closure of the Chaplygin cusp

$$
\mathrm{Im} \int_{\lambda_B}^{\lambda_D} \frac{dz}{d\lambda} d\lambda = 0.
$$

According to the free choice of the parameters $0 \le q_c < 1$, $q_h > 1$, there is a two parameter family of solutions, corresponding to differently shaped cusps in differently wide channels. Figure 3 is an example of solution relevant to the choice $q_c = 0.8$, $q_h = 3$. For $q_c \to 0$ the solution is the Pocklington infinite hollow shown in figure 7. For $q_h \to 1$, the channel width goes to infinity, that is, the solutions are relevant to a one-parameter (q_c) family of single bodies in an unbounded flow domain. These solutions can be obtained by considering that, in the above definition of $dw/d\lambda$, sources and sinks located in λ_A, $\lambda_{A'}$ and λ_G merge in a quadrupole located in $\lambda_A = \lambda_{A'} = \lambda_G = 0$; eq. 9 thus becomes

$$
\frac{dw}{d\lambda} = \frac{M}{2\pi} \left\{ \wp'(\lambda) + \frac{1}{2}Q_E/M[\zeta(\lambda - \lambda_E) - \zeta(\lambda)] + i\kappa \right\},
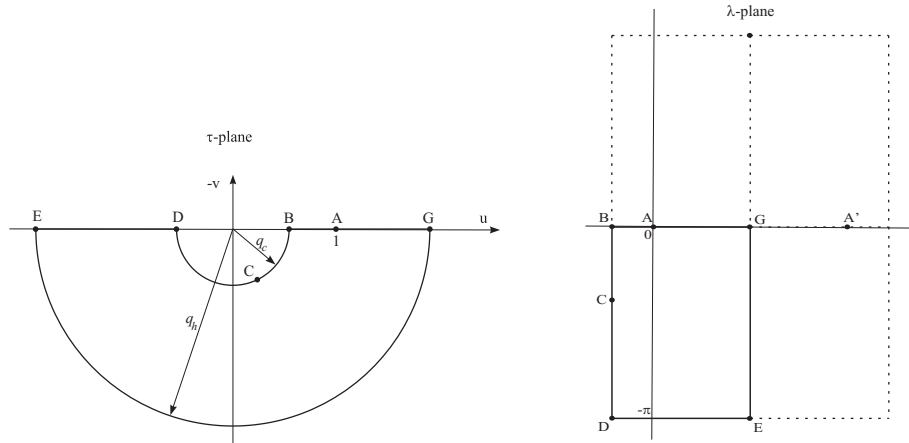$$

14

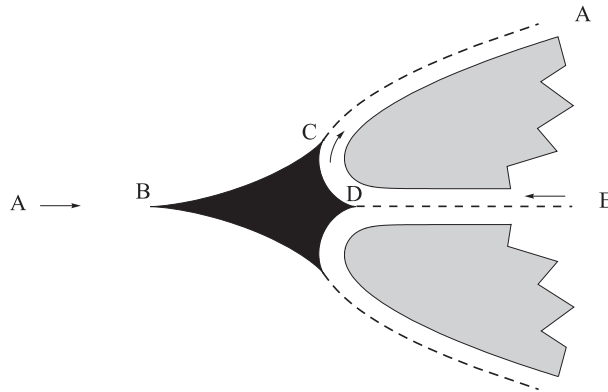Figure 13: Hodograph τ-plane and transformed λ-plane.

Figure 14: Chaplygin cusp in an unbounded domain ($q_c = 0.5$, $q_h = 1$).

where M is the quadrupole strength and $\wp'$ is the Weierstrass $\wp'$.

An example of solution is shown in figure 14, relevant to the choice $q_c = 0.5$.

4. Conclusions

As stated in [3], solid bodies free from adverse pressure gradients can be designed for the 2D inviscid flow, provided that some region of the flow field is affected by vorticity. Thus, bodies could be conceived which, by inducing a steady rotational separated flow, yield the conditions to be free from uncontrolled secondary separations. Despite the highly idealized flow

15

model, this idea is interesting in the field of flow control at high Reynolds number.

Following the same idea as in [4], examples of such bodies are here provided by the analytical tool of the hodograph-plane method. In [4] the separated flow was modeled by concentrating the vorticity into point vortices and the solid bodies were obtained by replacing the stagnation points of a vortex pair flow by Chaplygin cusps. The present paper adopts a different model for the separated flow, with the vorticity concentrated in vortex sheets bounding hollow regions.

In a way similar to [4], the stagnation points of the Pocklington [12] hollow vortex pair have been replaced by Chaplygin cusps. The resulting flow can be seen as the desingularization of the point vortices considered in [4] into hollow regions with growing area.

Moreover, by replacing the stagnation points of the infinite Pocklington hollows [12] with Chaplygin cusps, examples are provided of bodies with infinite open wakes.

The Pocklington solutions, which are pertinent to single region in an unbounded flow, have been generalized to flow inside a channel or, equivalently, to a cascade flow.

References

[1] F. G. Avhadiev and A. Maklakov. A theory of pressure envelopes for hydrofoils. *Ship Technology Res.*, 42:81–102, 1995.

[2] A. M. Elizarov, N. B. Il'inskiy, and A. V. Potashev. *Mathematical Methods of Airfoil Design.* Akademie Verlag, Berlin, 1997.

[3] S. I. Chernyshenko, B. Galletti, Iollo, A., and L. Zannetti. Trapped vortices and a favorable pressure gradient. *J. Fluid Mech.*, 482:235–255, 2003.

[4] L. Zannetti and S. Chernyshenko. Vortex pair and Chaplygin cusps. *Eur. J. Mech. B/Fluids*, 24:328–337, 2005.

[5] S. A. Chaplygin. *Collected Works Vol. 1, 5-18.* Gostekizdat, Moscow 1948.

[6] M. I. Gurevich. *Theory of Jets in Ideal Fluids.* Academic Press, 1965.

[7] G. K. Batchelor. On steady laminar flows with closed streamlines at large Reynolds number. *J. Fluid Mech.*, 1:177–190, 1956.

[8] G. K. Batchelor. A proposal concerning laminar wakes behind bluff bodies at large Reynolds number. *J. Fluid Mech.*, 1:388–398, 1956.

[9] S. I. Chernyshenko. Asymptotic theory of global separation. *Appl. Mech. Rev.*, 51:523–536, 1998.

[10] A. Elcrat, B. Fornberg, M. Horn, and K. Miller. Some steady vortex flows past a circular cylinder. *J. Fluid Mech.*, 409:13–27, 2000.

[11] F. Gallizio, A. Iollo, B. Protas, and L. Zannetti. On continuation of inviscid vortex patches . *Physica D*, 239:190–201, 2010.

[12] H. C. Pocklington. The configuration of a pair of equal and opposite hollow straight vortices, of finite cross-section, moving steadily through fluid. *Proc. Camb. Phil. Soc.*, 8:178–187, 1895.

[13] J. H Michell. On the theory of free stream lines. *Phil Trans. R. Soc. Lond. A*, 182:394–431, 1890.

[14] M. A. Lavrentiev. *Variational Methods for Boundary Value Problems for Systems of Elliptic Functions*. Noordhoff, 1962.

[15] A. Lin and L. Landweber. On a solution of the Lavrentiev wake model and its cascade. *J. Fluid Mech.*, 79:801–823, 1977.

[16] H. Telib and L. Zannetti. Hollow wakes past arbitrarily shaped obstacles. *J. Fluid Mech.*, 669:214–224, 2011.

[17] A. Elcrat and L. Zannetti. Models for inviscid wakes past a normal plate. *J. Fluid Mech.*, In press, 2012.

[18] S. G. Llewellyn Smith and D. G. Crowdy. Structure and stability of hollow vortex equilibria. *J. Fluid Mech.*, 691:170–200, 2012.

[19] D. G. Crowdy and C. C. Green. Analytical solution for von Karman streets of hollow vortices. *Phys. Fluids*, 23:126602, 2011.

[20] S. A. Tanveer. *Topics in 2-D separated vortex flows*. PhD Thesis, CALTECH, 1984.

[21] S. A. Tanveer. A steadily translating pair of equal and opposite vortices with vortex sheets on their boundaries. *Studies Apll. Math*, 74:139–154, 1986.